Application of a numerical model to simulate seasonal differences in onshore normalized wind profiles up to 160 m

Nissen, Jesper Nielsen; Gryning, Sven-Erik

Published in:
EWEC 2009 Proceedings online

Publication date:
2009

Document Version
Publisher's PDF, also known as Version of record

Citation (APA):
Nissen, J. N., & Gryning, S-E. (2009). Application of a numerical model to simulate seasonal differences in onshore normalized wind profiles up to 160 m. In *EWEC 2009 Proceedings online* EWEC.

APPLICATION OF A NUMERICAL MODEL TO SIMULATE SEASONAL DIFFERENCES IN ONSHORE NORMALIZED WIND PROFILES UP TO 160 M

Jesper Nielsen Nissen – Sven-Erik Gryning
Risoe-DTU National Laboratory for Sustainable Energy

Abstract

This work aims to study the seasonal difference in normalized wind speed above the surface layer as it is observed at the 160m high mast at the coastal site Høvsøre at winds from the sea (westerly). Normalized and stability averaged wind speeds above the surface layer are observed to be 20 to 50 % larger in the winter/spring seasons compared to the summer/autumn seasons at winds from west within the same atmospheric stability class.

A method combining the mesoscale model, COAMPS, and observations of the surface stability of the marine boundary layer is presented. The objective of the method is to reconstruct the seasonal signal in wind speed and identify the physical process behind. The method proved reasonably successful in capturing the relative difference in wind speed between seasons, indicating that the simulated physical processes are likely candidates to the observed seasonal signal in normalized wind speed.

Introduction

An increasing demand for the ability to estimate the wind climate above the surface layer in coastal regions has been generated by the wind power industry because of the steady increase of modern wind turbines with hub heights situated well above the surface layer height. To choose the optimal placement for a wind turbine, information about the wind energy potential needs to be properly assessed. The wind energy potential is proportional to cube of the wind speed at hub height, implying that even a small error in estimating the wind speed can have a large impact on the wind energy potential assessment. Conventional methods for assessing wind speed at heights of up to 200 m, such as that of Troen and Lundtang (1989), are derived from wind measurement taken close to the surface and extrapolated to greater heights by assuming a logarithmic increase of the wind speed with height, with a correction for stability effects.

$$U(z) = u_* \left[\frac{\ln(z/z_0)}{\kappa} + \psi\left(\frac{z}{L}\right) \right] \tag{1}$$

where

z=height, z_0=roughness lenght, u_*=friction velocity

κ=von Karman constant =0.4

ψ=empirical stability function following

Businger (1973); Dyer (1974) and L=Monin-Obukov length

The derivation of the logarithmic wind profile assumes homogeneous surface properties and a constant momentum flux and is therefore confined to the surface layer. Little is known about boundary layer wind profiles above the surface layer, but recent attempts to address this problem have been put forward by Högström et al. (2006) and Gryning et al. (2007), where extension to the Monin-Obukhov surface similarity scaling are suggested with some success.

In a coastal zone, the description of the vertical wind shear is complicated by non-homogenous upstream surface conditions, orography, change of roughness and heat capacity, all of which influence the vertical wind shear and are difficult to describe using simple, universal formulas. An alternative approach is adapted in this study where a well-validated mesoscale model is used to calculate the wind profile in the coastal region, resolving what is considered to be the main upstream physical processes. An observational study is performed in order to quantify how the upstream conditions influence the vertical wind shear close to the coastline, and the numerical simulations and observations are brought together to test the ability of the model to predict the vertical wind shear up to a height of 160 m at a distance of 1500 m downstream from a coastline.

The focus is on winds from the sea where a systematic over-speeding, compared to the traditional logarithmic wind profile, is observed at the top of the surface layer in the winter and spring months and likewise, a systematic under-speeding is found during summer and autumn. As this flow pattern is seasonally dependant, it is considered that heat exchange between the North Sea and the lower part of the atmospheric boundary layer plays a major role in the physical processes behind the observed structure of the wind profile. These processes are not accounted for in conventional wind energy potential assessment methods and the question posed here is:

Is a numerical model setup with a reasonable vertical resolution in the boundary layer able to reproduce the observed wind profiles and their seasonal variability, when only a limited number of physical surface processes are accounted for?

Observations

The observational basis for this work consists of measurements from the Høvsøre National Test Station for Large Wind Turbines situated in the northwestern part of Denmark (*Figure 1*). The data is gathered during the period from February 2004 to May 2008.

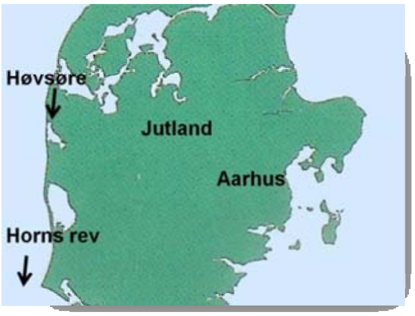

Figure 1: Høvsøre and Horns rev position

Upstream observations of the stability distribution in the marine boundary layer were found to be of importance in describing the seasonal differences in the normalized wind profiles at Høvsøre and measurements from offshore wind park Horns rev were therefore used. To classify the stability for the Høvsøre observations, the Monin-Obukhov length, L, defined in (2), is evaluated from the Høvsøre sonic anemometer mounted at 20 m height. The observations are subsequently sorted into 7 stability bins following Gryning et al. (2007) and normalized by the friction velocity at 20 m as defined in (3) and finally averaged according to season.

$$L = \frac{-u_{*20m}^{\;3}}{k\left(g/T_{20m}\right)\left(\overline{w'T'}\right)_{20m}} \qquad (2)$$

$\kappa =$ von Karman constant

$g =$ acceleration of gravity

$T =$ temperature

$$u_*^{\,2} = \left[\overline{u'w'_{20m}}^{\,2} + \overline{v'w'_{20m}}^{\,2}\right]^{0.5} \qquad (3)$$

The results from this procedure can be seen in Figure 2. It is here observed how the seasons wind speed systematically splits at heights above 40 m. The spring season is always the most windy (except from bin -500<L<-200 which is poorly represented for the winter season) and the autumn is the les windy season. Winter and summer follows systematically in between the spring and autumn seasons for all stability bins.¨

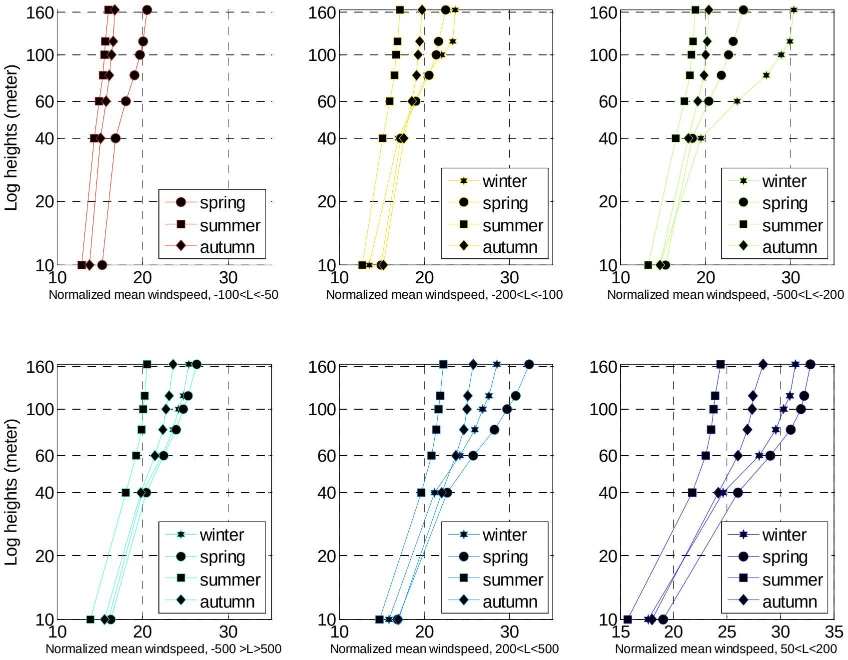

Figure 2:Stability-bin-averaged and normalized wind profiles for each season

Method and physical process

A method to reveal the underlying physical process behind the seasonal signal is presented. A well-validated numerical model is used as a numerical laboratory in an idealized configuration aiming at keeping the boundary layer process under easy control.

It is posed that an observed phase shift in annual stability distribution between, in Figure 3 the coastal station Høvsøre and in Figure 4 the upstream marine station Horns rev, is the main physical process. A numerical experiment is designed in order to test this accordingly.

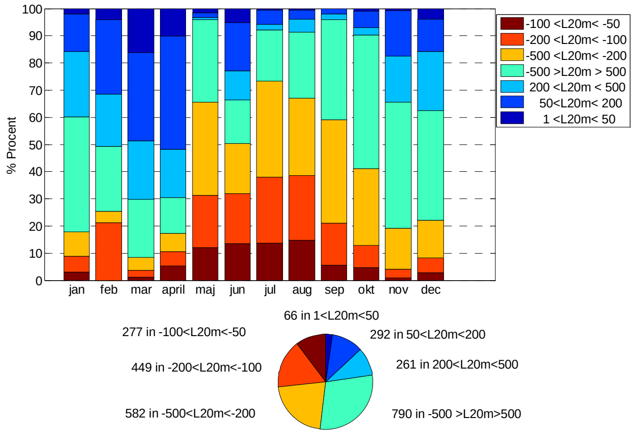

Figure 3 Høvsøre test station: monthly stability distribution (bar graph, upper) and yearly distribution of the stability distribution (pie chart, lower). Left hand integers denote number of observation in stability class (legend, lower)

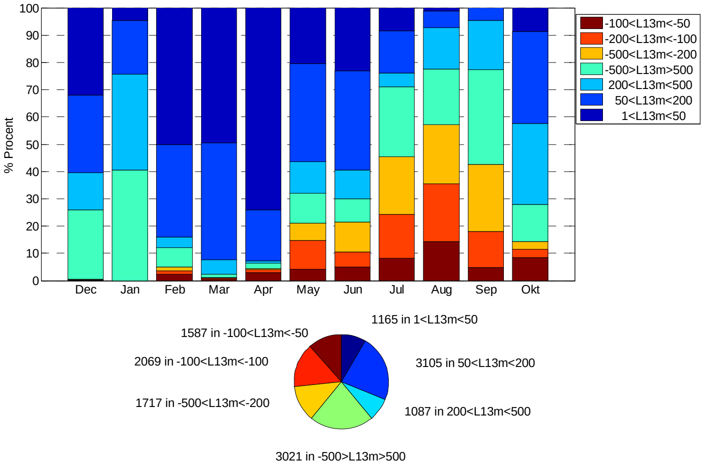

Figure 4 Horns Rev wind farm: monthly stability distribution (bar graph, upper) and yearly distribution of the stability distribution (pie chart, lower). Left hand integers denote number of observation in stability class (legend,

lower). The data is from the period December 2003 to November 2004, for the 225°-315° wind direction sector. L is calculated from the bulk Richardson number (4) *and* (5), *following Grachev and Fairall (1996)*

$$Ri_b = \frac{gz\left(\Delta\theta\right)_{13m-(-4m)}}{\theta_{13m}{u_{15m}}^2} \qquad (4)$$

$$(5) \qquad \frac{z}{L} = C_1 Ri_b \quad \text{Unstable} \qquad \frac{z}{L} = \frac{C_2 Ri_b}{1 - C_3 Ri_b} \quad \text{Stable}$$

Modeling and result:

The numerical experiment consists of 2 sets of simulations. First 18 Marine boundary layers (MABL) are created, this is step 1. In this step, air is allowed 6 different initial temperatures and is swept across a sea surface, which is kept at temperature 277 K. The initial speed of the wind is varied from 10 m/s over 15 to 20 m/s and is initially constant with height. The marine atmospheric boundary layer is then spun up by the model and profiles of wind and temperature in equilibrium with the sea surface is generated during the 6 hours of integration time which is done with periodic boundary conditions. These 18 MABL are hereafter exposed to a cost line with 4 different temperatures - this is step 2. The end result of these two simulation steps is 72 simulations, where wind profiles are extracted from at a position relating to Høvsøre in terms of distance from the coast.

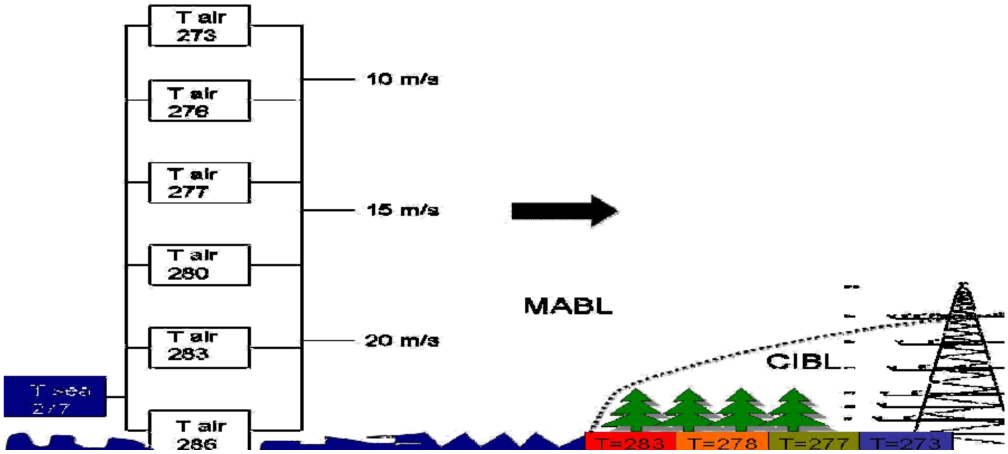

Figure 5: Conceptual model of the numerical experiment

To make the extracted profiles comparable to the observations from Høvsøre, an averaging procedure reflecting the particular season is needed. It is here posed that the physical process behind the seasonality in the normalized wind profiles, is the phase shift in the annual stability distribution (Figure 3 and Figure 4) and, this observed physical property of the North Sea climate, is therefore used to average the profiles in the following way. Each extracted wind profiles is assigned a weight for each season reflecting how often the MABL it originates from, occurs in that given season. The seasonal weights are attained by assumed that a MABL is fully characterised by the computed surface L. The probability/weight of the MABL in a given season is then the same as the probability of the computed L to occur in that season divided by the number of simulated MABL with the same L. The weight of each MABL for each season, depicted in Figure 6 is then used to average the normalized wind profiles within each stability bin. This result in one wind profiles for each season and stability bin, as depicted in

Figure 7 ad 8 which is then immediately comparable to the observed wind profiles from Høvsøre (Figure 7).

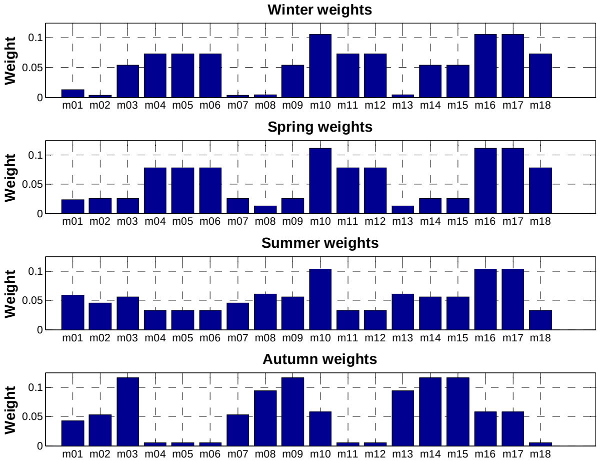

Figure 6 Seasonal weighs for the generated MABL. The syntax for the MABL is listed in appendix Table 1

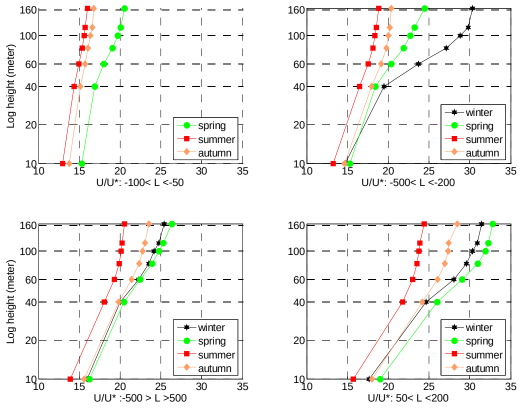

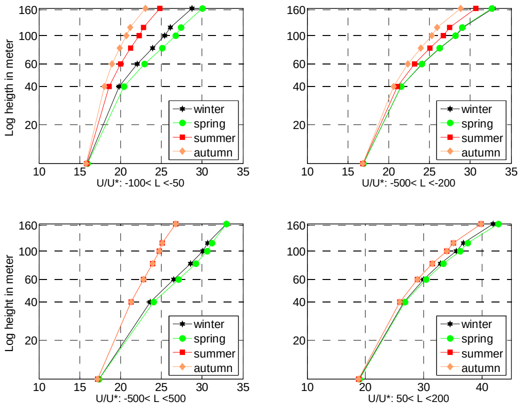

Figure 7: Observations *Figure 8: Simulations*

Results and conclusions:

The seasonal pattern as seen in figure 2 and 7 is to some extent reproduced by the method as seen in figure 8. The relatively larger wind speeds observed in spring and winter is clearly detectable in all 4 simulated stability bins. Also the trend towards higher wind speed at the top of the seasonal averaged profile with increasing stability is clearly seen. The height of the equilibrium layer is also seen to be captured quite well to 40 m the bin averaged seasonal profiles.

The experiment proved skill in predicting the seasonality in the normalized wind profiles for Høvsøre when incorporating information on the upstream stability distribution. Using the time lag in stability distribution in terms of L between the North Sea and Høvsøre made it possible to partial reproduce the observed seasonality indicating the some of the important physical processes behind the observation are captured in the idealized setup presented here. The observed normalized bin averaged wind profiles are, to a reasonable degree, seen to follow the conceptual model suggested by Sempreviva (1990); Jensen and Peterson (1977). The wind profiles from 100 m and up are characterized by a smaller slope and according Sempreviva (1990) and Jensen and Peterson (1977) can the smaller slope be interpreted as an equilibrium with the upstream smoother sea surface. This feature is not captured in the numerical setup and the upper part of the simulated bin averaged wind profile is seen to be over predicted for all seasons and bins. The difference between the simulations and the observations for wind speed above 100m clearly shows that the highly idealized simulations utilities here, does not capture correctly the boundary layer processes, responsible for the MABL structures over the North Sea as seen in the observations above 100m.

The most likely explanation for this mismatch between the observations and the simulations is a possible too low simulated height of the averaged upstream constant flux layer. The conceptual model suggested by Sempreviva (1990) and Jensen and Peterson (1977) assumes logarithmic upwind wind profile dictating a upwind average constant flux layer height of at least 160 m in order to diagnose the characteristically kink feature in the wind profile as seen in the observations from Høvsøre.

Model skills relative comparison

An increase in agreement between the observations and the simulations are found when comparing the relative differences, denoted RD, calculated as outlined in (6), (7) and depicted in Figure 9.

The 100 m height is chosen for a number of reasons. The most important one is that it relates to the height of the internal boundary layer at the position of the observations mast and therefore reflects both local and upstream properties.

Bin 1: $-100< L < -50$

Good agreement is found between simulations and observations for the most convective bin where both spring and summer seasons are well predicted as seen in Figure 9. No observations were available from the winter season.

Observed relative difference at 100m between spring and the low wind season, is 24 % while the simulation gave 26 % while the season with the lowest relative difference was observed to be autumn with 4.8 and simulation gave 7.8.

The ratio between simulated relative spring-summer and relative simulated summer-autumn values is also in good agreement with the observed ratio of relative spring-autumn and summer-autumn values as seen in Figure 9. This result is encouraging as both observation and simulation are well presented in this stability bin as can be seen from Figure 9

Bin 3: $-500< L < -200$

The observed seasonal signal is under predicted by a factor of two in the slightly convective stability class. However is the factor two ratio between spring-summer and autumn-summer captured very well by the simulation as seen in Figure 9. It's worth noting that this stability class has 8 simulated profiles are therefore not as well represented in the simulations Figure 9 compared to bin 1, bin 4 and bin 7

Bin 4:$-500> L > 500$

For the neutral stability class good agreement is again found where both the observations and simulation are well presented. The simulated relative spring departure can be seen to be 25 % while the observed spring departure reads 20 %.

The winter season is also captured well by the simulations with a simulated relative departure of 23% and the observed relative departure reads 19 %. However is the summer season seen to be under predicted as the simulation reads only 2.9 % while observations show 12.5 %.

Bin $50< L < 200$

Bin 6 is under predicted by the simulations with nearly a factor of two for all seasons – however is the ratio among the seasonal relative departures is capture well by the simulations as seen Figure 9. Bin 6 has like bin 3, 8 simulated profiles and therefore among the stability class with the poorest representations by simulated profiles

Bin 7 $1< L < 50$

This stability class is rare at Høvsøre and only a few observations exist for the 4 year period spanned by the observations. Winter is the best represented season with 12 observations existing for this season while 6 observations can be found to represent the low wind summer season. Care must therefore be taken in the interpretation and evaluation of the model skill for this stability class as the observations are poorly represented. However do the simulations predict a relative departure for the winter season of 39% while the observations show 51 %.

The most stable stability class is the class with the most extreme difference in normalized wind speed at 100 and agreement on this feature is found between the simulations and the observations.

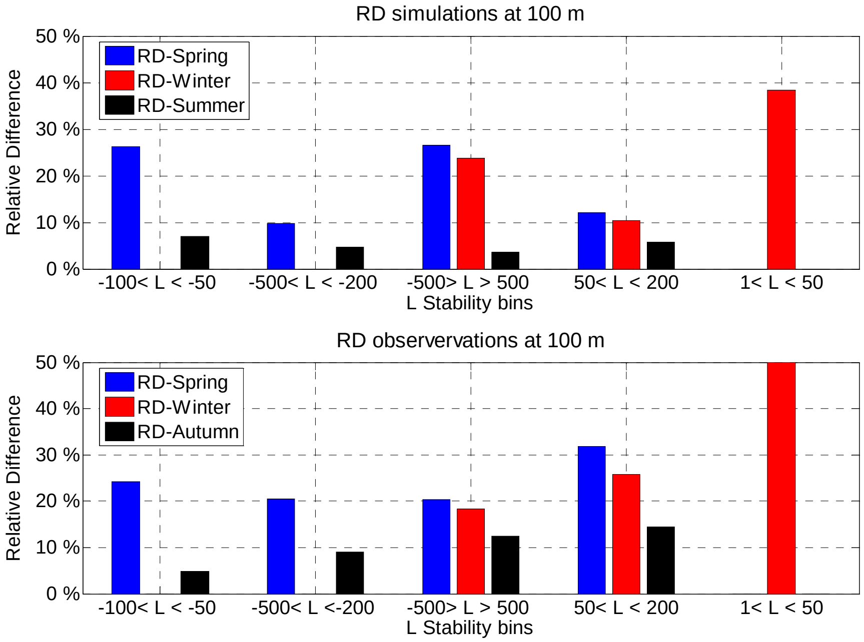

Figure 9 Simulated and observed relative difference between seasons at 100 m found according to (6) *and* (7)

$$\text{RD-winter} = \frac{\left[\text{Winter}\_Wspd_{100m} - Summer\_Wspd_{100m}\right]}{Summer\_Wspd_{100m}}100 \qquad (6)$$

Simulated profiles

$$\text{RD-winter}= \frac{\left[\text{Winter}\_Wspd_{100m} - Autumn\_Wspd_{100m}\right]}{Autumn\_Wspd_{100m}}100 \qquad (7)$$

Observed profiles

References

Grachev, A. and Fairall, C. (1996) “Dependence of the Monin-Obukhov stability parameter on the Bulk Richardson number over the Ocean” J. of Appl. Meteorol. **36** pp 406-414

Gryning, S.E., Batcvarova, E., Brümmer, B., Jørgensen, H. E. and Larsen, S, E (2007) “On the extension of the wind profile over homogeneous terrain beyond the surface layer” Boundary-Layer Meteorol. **124** pp 251-268

Hodur, R. M. (1997) “The Naval Research Laboratory’s coupled Ocean/atmosphere meso scale predition system (COAMPS)” Monthly Weather Review **125** pp 1414-1430

Hodur, R. M., and Doyle, J. D. 1998, “ The coupled ocean/atmosphere model prediction system COAMPS ”. Coastal ocean predict . Coastal and Estuarine stud. **56** pp 125-155

Högström, U., Smedman, A., and Bergström, H. (2006) ”Calculation of the wind speed variation with height over the sea” Wind Engineering **30** pp 269-286

Jensen N. O. and Peterson, E.W.,(1976) “ Wind flow near the surface of non uniform terrain” Report of progress for the year 1976 Progress report for U.S army grant available at Risø National Laboratory

Klemp, J. B., and Wilhelmson, R. B., (1977) “The simulation of there-dimensional convective storm dynamics” J. Atoms. Sci. **35** pp 1070-1096

Sempreviva, A. M. (1990) “Response of neutral boundary layers to change in Roughness” Boundary-Layer Meteorol. 50 pp 205-225

Troen, I., and Lundtang Petersen, E., (1989) “European Wind Atlas” Risø National Laboratory, Risø, Denmark

Appendix

Model Details

COAMPS is a finite-difference approximation to the non-hydrostatic fully compressible equations of motion following Klemp and Wilhemson (1977) with a suite of physical parameterizations of surface fluxes, boundary layer physics and moist processes described in Hodur (1997) and Hodur and Doyle (1998). The physical processes behind the parameterizations can be switched on and off in order to meet the complexity of the area of interest in the numerical experiment.

The model PBL scheme consists of a 1.5 order, level 2.5 closure scheme (Mellor & Yamada 1982) – A Louis 1979 surface layer scheme and a mixing length formulation following Blackadar (1962)

Table 1Syntax for the simulated MABL listed in figure 6

MABL nr	***m01***	***m02***	***m03***	***m04***	***m05***	***m06***	***m07***	***m08***	***M09***
Wspd	10	10	10	10	10	10	15	15	15
Air tmp Kelvin	273	276	277	280	283	286	273	276	277
MABL nr	***m10***	***m11***	***m12***	***m13***	***m14***	***m15***	***m16***	***m17***	***m18***
Wspd m/s	15	15	15	20	20	20	20	20	20
Airtmp Kelvin	280	283	286	273	276	277	280	283	286